Polarization Observables in Vector Meson Photoproduction from the FROST Experiment using CLAS at Jefferson Lab

Priyashree Roy

Florida State University

Dissertation Defense

11/01/2016

Outline

Outline

Understanding Hadrons

- Matter that we see around us is made up of hadrons like protons and neutrons. Hadrons are made of quarks and gluons which interact via the strong force.
- Six known quarks, each with a unique ‘flavor’ quantum number.
- Broad classification of hadrons:
  Baryons: 3 quarks, **Mesons**: quark-antiquark pairs.
- Gluons, the mediators of the strong force, also carry color charge. They participate in the strong interaction in addition to mediating it unlike photons in QED.

Understanding Hadrons

- Matter that we see around us is made up of hadrons like protons and neutrons. Hadrons are made of quarks and gluons which interact via the strong force.
- Six known quarks, each with a unique 'flavor' quantum number.
- Broad classification of hadrons:
  Baryons: 3 quarks, **Mesons**: quark-antiquark pairs.
- Gluons, the mediators of the strong force, also carry color charge. They participate in the strong interaction in addition to mediating it unlike photons in QED.

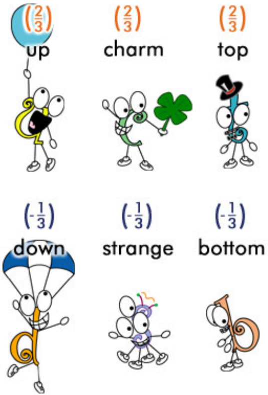

Understanding Hadrons

- Matter that we see around us is made up of hadrons like protons and neutrons. Hadrons are made of quarks and gluons which interact via the strong force.
- Six known quarks, each with a unique ‘flavor’ quantum number.
- Broad classification of hadrons:
  Baryons: 3 quarks, **Mesons**: quark-antiquark pairs.
- Gluons, the mediators of the strong force, also carry color charge. They participate in the strong interaction in addition to mediating it unlike photons in QED.

Baryons

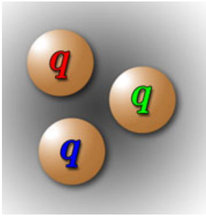

Mesons

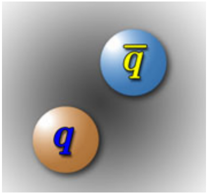

Understanding Hadrons

- Matter that we see around us is made up of hadrons like protons and neutrons. Hadrons are made of quarks and gluons which interact via the strong force.
- Six known quarks, each with a unique 'flavor' quantum number.
- Broad classification of hadrons:
  Baryons: 3 quarks, **Mesons**: quark-antiquark pairs.
- Gluons, the mediators of the strong force, also carry color charge. They participate in the strong interaction in addition to mediating it unlike photons in QED.

Baryons

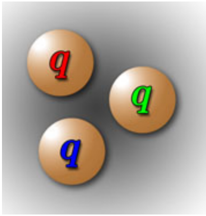

Mesons

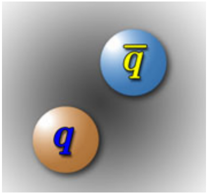

Understanding Hadrons

Quantum Chromodynamics (QCD) is the theory of the strong force which describes quark-gluon interactions. Two peculiar features of the strong force are:

Confinement ..

Asymptotic freedom ..

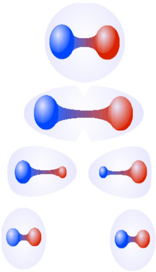

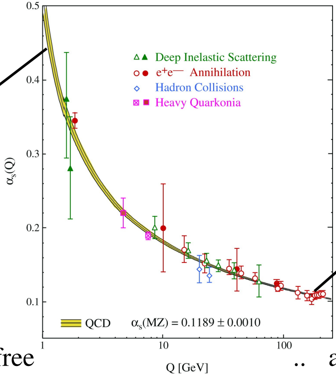

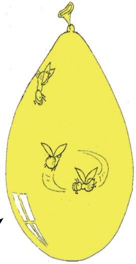

.. at large distances. No free quarks! Non-perturbative regime.

.. at short distances, as if the quarks were free.

S. Bethke, Prog. Part. Nucl. Phys. **58**, 351 (2007)

Baryon Spectroscopy

Open questions in the non-perturbative regime (where QCD is difficult to solve):
How does QCD give rise to excited hadrons?

- What is the origin of confinement? How are confinement and chiral symmetry breaking connected?
- What are the relevant degrees of freedom? How do they evolve with energy?

Baryon Spectroscopy

Open questions in the non-perturbative regime (where QCD is difficult to solve): How does QCD give rise to excited hadrons?

- What is the origin of confinement? How are confinement and chiral symmetry breaking connected?
- What are the relevant degrees of freedom? How do they evolve with energy?

Baryon Spectroscopy

Open questions in the non-perturbative regime (where QCD is difficult to solve):
How does QCD give rise to excited hadrons?

- What is the origin of confinement? How are confinement and chiral symmetry breaking connected?
- What are the relevant degrees of freedom? How do they evolve with energy?

Baryon Spectroscopy

Open questions in the non-perturbative regime (where QCD is difficult to solve):
How does QCD give rise to excited hadrons?

- What is the origin of confinement? How are confinement and chiral symmetry breaking connected?
- What are the relevant degrees of freedom? How do they evolve with energy?

Baryon spectroscopy, a tool to understand the effective degrees of freedom in excited baryons: map out the spectrum and study the underlying pattern.
This dissertation focuses on the spectrum of light baryons containing u and d quarks.
Symbol: N if $I = 1/2$, Δ if $I = 3/2$.
Nomenclature: Symbol (Mass in MeV/c^2) J^P

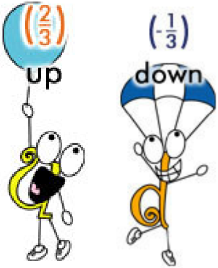

Light Baryon Spectroscopy

Effective degrees of freedom

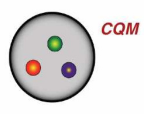

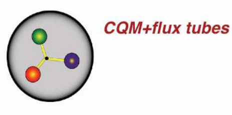

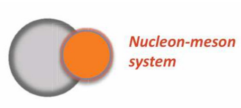

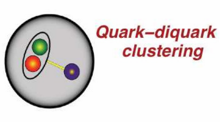

+ Lattice-QCD computations
(complementary to phenomenological models)

Map out the excited states of (light) baryons, identify the underlying multiplets to get an insight into the effective degrees of freedom.

Understanding the Light Baryon Spectrum

- **Underlying Pattern**: the resonances can be grouped into bands and multiplets.
- The level counting in LQCD for each J^P in each band is **consistent** with CQM.

A CQM prediction for N*

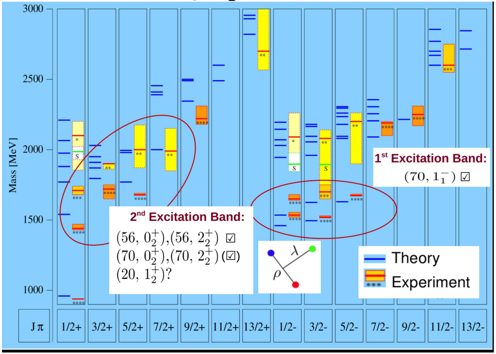

S. Capstick and N. Isgur, Phys. Rev. D **34** (1986) 2809

N* from Lattice-QCD

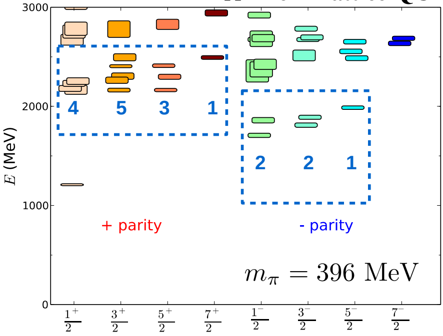

R. Edwards *et al.* Phys. Rev. D **84** 074508 (2011)
Picture courtesy V. Bukert (CLAS collaboration meeting 2015)

Understanding the Light Baryon Spectrum

- Many **'missing'** states, particularly above 1.7 GeV in W.
- **A possible explanation**: perhaps the static quark-diquark picture is correct?

A CQM prediction for N*

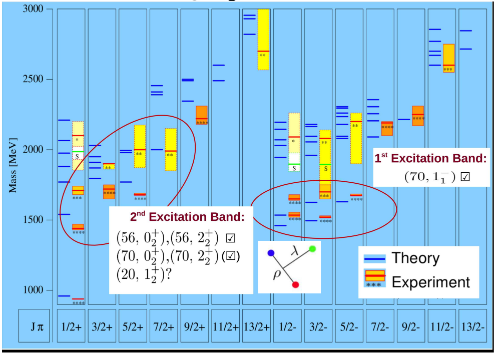

S. Capstick and N. Isgur, Phys. Rev. D **34** (1986) 2809

N* from Lattice-QCD

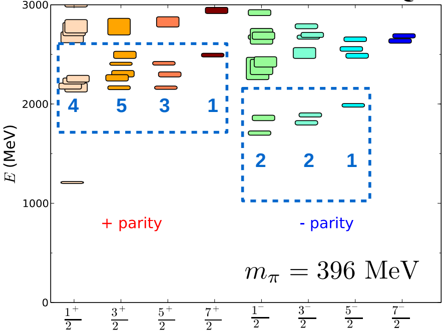

R. Edwards *et al.* Phys. Rev. D **84** 074508 (2011)
Picture courtesy V. Bukert (CLAS collaboration meeting 2015)

Understanding the Light Baryon Spectrum

- N(1900)3/2$^+$ (which can be assigned as a member of the quartet of (**70**, 2_2^+)) cannot be accommodated in the naive quark-diquark picture, both oscillators need to be excited.
- No sign of 'freezing' in LQCD calculations.

A CQM prediction for N*

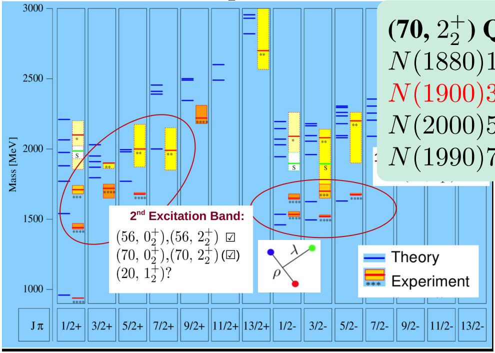

(70, 2_2^+) Quartet
$N(1880)1/2^+$ $**$
$N(1900)3/2^+$ $***$
$N(2000)5/2^+$ $**$
$N(1990)7/2^+$ $**$

N* from Lattice-QCD

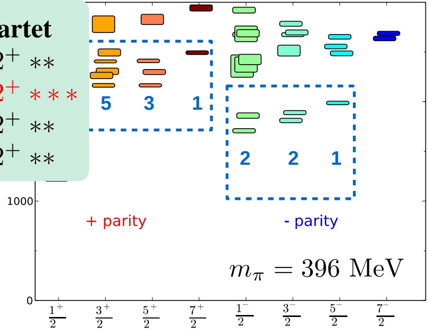

Bradford *et al.* (CLAS), PRC **75**, 035205 (2007), Observables C_x, C_z from $\vec{\gamma}p \to K^+\vec{\Lambda}$
Fits: BnGa Model, V.A. Nikonov *et al.*, Phy. Lett. B **662**, 245 (2008)

Understanding the Light Baryon Spectrum

- Many **'missing'** states, particularly above 1.7 GeV in W.
- ~~**A possible explanation**: perhaps the static quark-diquark picture is correct?~~

A CQM prediction for N*

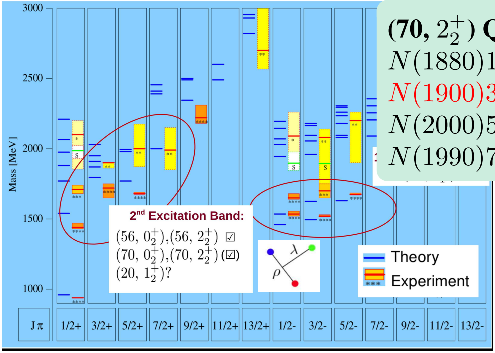

$(70, 2_2^+)$ Quartet
$N(1880)1/2^+$ $**$
$N(1900)3/2^+$ $***$
$N(2000)5/2^+$ $**$
$N(1990)7/2^+$ $**$

N* from Lattice-QCD

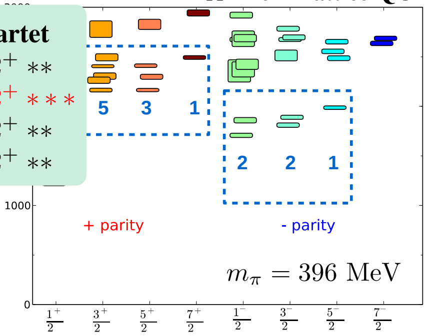

Bradford *et al.* (CLAS), PRC **75**, 035205 (2007), Observables C_x, C_z from $\vec{\gamma} p \to K^+ \vec{\Lambda}$
Fits: BnGa Model, V.A. Nikonov *et al.*, Phy. Lett. B **662**, 245 (2008)

Vector Meson and Multi-Pion Photoproduction

Alternate explanation suggested from an experimental point-of-view:

- Past measurements were mostly done using π beams. It is predicted that the high-mass resonances predominantly couple to γ beams.
- The high-mass resonances preferably decay to heavier mesons, e.g. vector mesons (e.g. ω, ρ, ϕ), or sequentially decay to multi-particle final states via intermediate resonances.
- The study these reactions also aid in further investigating poorly-understood properties of known resonances. Their contributions to these reactions have mostly remained under-explored.
- These factors motivated the analysis of $\gamma p \to p\pi^+\pi^-$ and $\gamma p \to p\omega \to p\pi^+\pi^-(\pi^0)$ reactions. The former gives information on $N^* \to p\rho$, and on sequential decays via intermediate resonances.

Vector Meson and Multi-Pion Photoproduction

Alternate explanation suggested from an experimental point-of-view:

- Past measurements were mostly done using π beams. It is predicted that the high-mass resonances predominantly couple to γ beams.
- The high-mass resonances preferably decay to heavier mesons, e.g. vector mesons (e.g. ω, ρ, ϕ), or sequentially decay to multi-particle final states via intermediate resonances.
- The study these reactions also aid in further investigating poorly-understood properties of known resonances. Their contributions to these reactions have mostly remained under-explored.
- These factors motivated the analysis of $\gamma p \to p\pi^+\pi^-$ and $\gamma p \to p\omega \to p\pi^+\pi^-(\pi^0)$ reactions. The former gives information on $N^* \to p\rho$, and on sequential decays via intermediate resonances.

Vector Meson and Multi-Pion Photoproduction

Alternate explanation suggested from an experimental point-of-view:

- Past measurements were mostly done using π beams. It is predicted that the high-mass resonances predominantly couple to γ beams.
- The high-mass resonances preferably decay to heavier mesons, e.g. vector mesons (e.g. ω, ρ, ϕ), or sequentially decay to multi-particle final states via intermediate resonances.
- The study these reactions also aid in further investigating poorly-understood properties of known resonances. Their contributions to these reactions have mostly remained under-explored.
- These factors motivated the analysis of $\gamma p \to p\pi^+\pi^-$ and $\gamma p \to p\omega \to p\pi^+\pi^-(\pi^0)$ reactions. The former gives information on $N^* \to p\rho$, and on sequential decays via intermediate resonances.

Particle J^P	overall	Status as seen in $N\gamma$	$N\pi$	$N\eta$	$N\sigma$	$N\omega$	ΛK	ΣK	$N\rho$	$\Delta\pi$
$N(1700)\ 3/2^-$	***	**	***	*			*	*	*	***
$N(1710)\ 1/2^+$	****	****	****	***		**	****	**	*	**
$N(1720)\ 3/2^+$	****	****	****	***			**	**	**	*
$N(1860)\ 5/2^+$	**		**						*	*
$N(1875)\ 3/2^-$	***	***	*			**	***	**		***
$N(1880)\ 1/2^+$	**	*	*		**		*			
$N(1895)\ 1/2^-$	**	**	*	**			**	*		
$N(1900)\ 3/2^+$	***	***	**	**		**	***	**	*	**
$N(1990)\ 7/2^+$	**	**	**					*		
$N(2000)\ 5/2^+$	**	**	*	**			**	*	**	
$N(2040)\ 3/2^+$	*		*							
$N(2060)\ 5/2^-$	**	**	**	*				**		
$N(2100)\ 1/2^+$	*		*							
$N(2120)\ 3/2^-$	**	**	**				*	*		
$N(2190)\ 7/2^-$	****	***	****			*	**		*	
$N(2220)\ 9/2^+$	****		****							
$N(2250)\ 9/2^-$	****		****							
$N(2300)\ 1/2^+$	**		**							
$N(2570)\ 5/2^-$	**		**							

Particle Data Group 2016

Vector Meson and Multi-Pion Photoproduction

Alternate explanation suggested from an experimental point-of-view:

- Past measurements were mostly done using π beams. It is predicted that the high-mass resonances predominantly couple to γ beams.
- The high-mass resonances preferably decay to heavier mesons, e.g. vector mesons (e.g. ω, ρ, ϕ), or sequentially decay to multi-particle final states via intermediate resonances.
- The study these reactions also aid in further investigating poorly-understood properties of known resonances. Their contributions to these reactions have mostly remained under-explored.
- These factors motivated the analysis of $\gamma p \to p\pi^+\pi^-$ and $\gamma p \to p\omega \to p\pi^+\pi^-(\pi^0)$ reactions. The former gives information on $N^* \to p\rho$, and on sequential decays via intermediate resonances.

		Status as seen in								
Particle J^P	overall	$N\gamma$	$N\pi$	$N\eta$	$N\sigma$	$N\omega$	ΛK	ΣK	$N\rho$	$\Delta\pi$
$N(1700)\,3/2^-$	***	**	***	*			*	*	*	***
$N(1710)\,1/2^+$	****	****	****	***		**	****	**	*	**
$N(1720)\,3/2^+$	****	****	****	***			**	**	**	*
$N(1860)\,5/2^+$	**		**						*	*
$N(1875)\,3/2^-$	***	***	*			**	***	**		***
$N(1880)\,1/2^+$	**	*	*		**		*			
$N(1895)\,1/2^-$	**	**	*	**			**	*		
$N(1900)\,3/2^+$	***	***	**	**		**	***	**	*	**
$N(1990)\,7/2^+$	**	**	**					*		
$N(2000)\,5/2^+$	**	**	*	**			**	*	**	
$N(2040)\,3/2^+$	*		*							
$N(2060)\,5/2^-$	**	**	**	*				**		
$N(2100)\,1/2^+$	*		*							
$N(2120)\,3/2^-$	**	**	**				*	*		
$N(2190)\,7/2^-$	****	***	****			*	**		*	
$N(2220)\,9/2^+$	****		****							
$N(2250)\,9/2^-$	****		****							
$N(2300)\,1/2^+$	**		**							
$N(2570)\,5/2^-$	**		**							

Particle Data Group 2016

Why are Spin Observables Important?

Atomic Cross Section

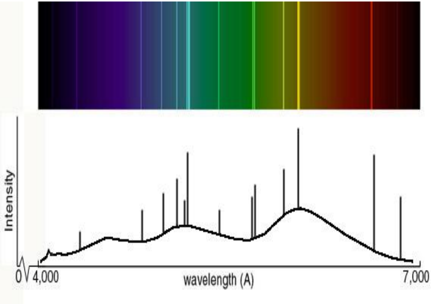

Baryon Cross Section

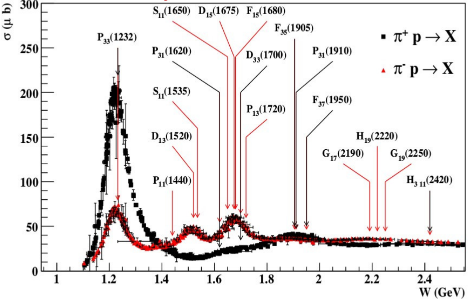

(Courtesy of Michael Williams)

- Baryon resonances are broad and overlapping so ‘peak-hunting’ is not a good way to look for resonances.
- Significant background from non-resonant processes which are entangled with resonant processes.

Why are Spin Observables Important?

Polarized measurements in addition to the unpolarized cross section measurements necessary to disentangle and reveal the resonances with minimum ambiguities.

Why are Spin Observables Important?

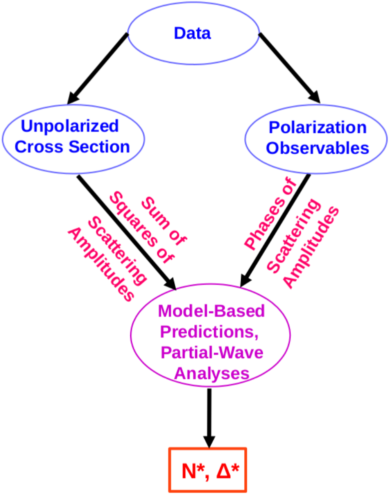

Polarized measurements in addition to the unpolarized cross section measurements necessary to disentangle and reveal the resonances with minimum ambiguities.

Spin Observables for $\vec{\gamma}\vec{p} \to p\pi^+\pi^-$ & $p\omega$ @ CLAS

The FROST N^* Program in Hall B, JLab

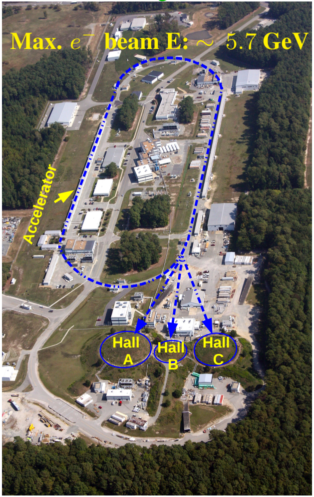

$\vec{\gamma}\vec{p} \to p\omega$

Beam \ Target	Transversely Pol.	Longitudinally Pol.
Linearly Pol.	Σ, T, H, P	Σ, G
Circularly Pol.	F, T	E

$\vec{\gamma}\vec{p} \to p\pi^+\pi^-$

Beam \ Target	Transversely Pol.	Longitudinally Pol.
Linearly Pol.	$P^{s,c}_{x,y}$, $P_{x,y}$, $I^{s,c}$	$P^{s,c}_{z}$, P_z, $I^{s,c}$
Circularly Pol.	$P^{\odot}_{x,y}$, $P_{x,y}$, $I^{\odot}$	$P^{\odot}_{z}$, P_z, $I^{\odot}$

13 spin observables extracted in this analysis
(Analysis **approved** by the CLAS collaboration)
Data acquired
Final or prelim. results available

Spin Observables for $\vec{\gamma}\vec{p} \to p\pi^+\pi^-$ & $p\omega$ @ CLAS

$$\sigma_{\text{total}} = \sigma_0[1 - \mathbf{\Sigma}\,\delta_l \cos(2\phi) + \Lambda\cos(\alpha)(-\delta_l\,\mathbf{H}\sin(2\phi) + \delta_\odot\,\mathbf{F}) - \Lambda\sin(\alpha)(-\mathbf{T} + \delta_l\,\mathbf{P}\cos(2\phi)) - \Lambda_z(-\delta_l\,\mathbf{G}\sin(2\phi) + \delta_\odot\,\mathbf{E})]$$

$\delta_\odot(\delta_l)$: degree of beam polarization
Λ : degree of target polarization

$\vec{\gamma}\vec{p} \to p\omega$

Beam \ Target	Transversely Pol.	Longitudinally Pol.
Linearly Pol.	Σ, T, H, P	Σ, G
Circularly Pol.	F, T	E

$\vec{\gamma}\vec{p} \to p\pi^+\pi^-$

Beam \ Target	Transversely Pol.	Longitudinally Pol.
Linearly Pol.	$P^{s,c}_{x,y}$, $P_{x,y}$, $I^{s,c}$	$P^{s,c}_z$, P_z, $I^{s,c}$
Circularly Pol.	$P^{\odot}_{x,y}$, $P_{x,y}$, $I^{\odot}$	$P^{\odot}_z$, P_z, $I^{\odot}$

13 spin observables extracted in this analysis
(Analysis **approved** by the CLAS collaboration)
Data acquired
Final or prelim. results available

The FROST Experiment using CLAS at JLab

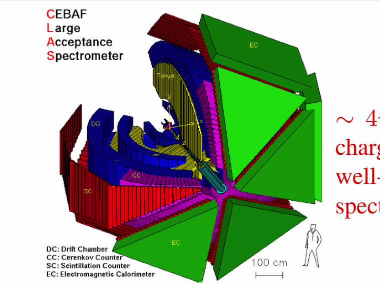

$\sim$ 4π acceptance of charged particles, well-suited for spectroscopy.

Coherent edges: 0.9-2.1 GeV (0.2 GeV wide)

Deg. of linear beam pol., δ_γ: $40 - 60\%$

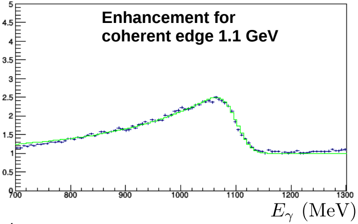

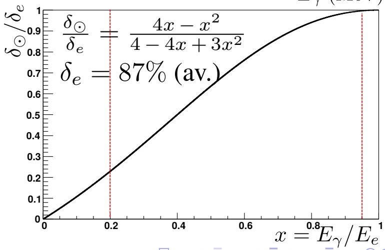

g9b run (Mar to Aug, 2010)

Photon Pol.: Linear/Circular

Target: (Nitroxyl) Doped Butanol (C_4H_9OH)

Target Pol.: Transverse

W **range:** 1.4-2.1 GeV (Lin. Data)
1.5-2.5 GeV (Circ. Data)

The FROzen Spin Target (FROST) Apparatus

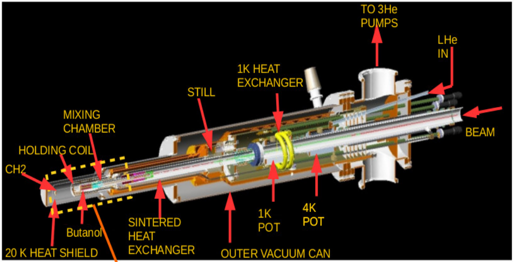

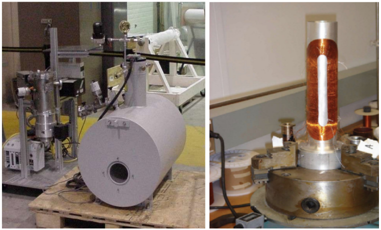

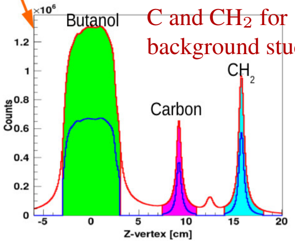

C and CH_2 for background studies

- Polarizing field = 5 T, T~ 0.3 K
- Dipole holding field = 0.5 T, T~ 50 mK
- Offset angle = 116.1 ± 0.4° from x_{lab}
- Av. target pol. = 81.0 ± 1.7%
- Relaxation time: 3400 hrs w/ beam, 4000 hrs w/o beam

Outline

Data Selection and Analysis

- **Topologies for $p\pi^+\pi^-$:**
  $\vec{\gamma}\vec{p} \to p\pi^+$ (missing π^-)
  $\vec{\gamma}\vec{p} \to p\pi^-$ (missing π^+)
  $\vec{\gamma}\vec{p} \to p\pi^+\pi^-$ (no missing particle)
  The observables are weighted avg. over topologies.
- **Topology for $p\omega$ (89% branching fraction):**
  $\vec{\gamma}\vec{p} \to p\pi^+\pi^-$(missing π^0)
  Topology identified using Kinematic fitting.
- **Standard cuts & corrections:** vertex cut, photon selection, β cuts, E-p corrections.
- **Event-based method**[1] for signal-background separation.
- **Event-based maximum likelihood method**[2] to fit angular distributions in $\phi_{\mathrm{lab}}^{\mathrm{recoil}}$ and extract the polarization observables.

Data Selection and Analysis

- **Topologies for** $\mathrm{p}\pi^+\pi^-$:
  $\vec{\gamma}\vec{p} \to p\pi^+$ (missing π^-)
  $\vec{\gamma}\vec{p} \to p\pi^-$ (missing π^+)
  $\vec{\gamma}\vec{p} \to p\pi^+\pi^-$ (no missing particle)
  The observables are weighted avg. over topologies.
- **Topology for** $\mathrm{p}\omega$ **(89% branching fraction):**
  $\vec{\gamma}\vec{p} \to p\pi^+\pi^-$(missing π^0)
  Topology identified using Kinematic fitting.
- **Standard cuts & corrections:** vertex cut, photon selection, β cuts, E-p corrections.
- **Event-based method**[1] for signal-background separation.
- **Event-based maximum likelihood method**[2] to fit angular distributions in $\phi^{\mathrm{recoil}}_{\mathrm{lab}}$ and extract the polarization observables.

Data Selection and Analysis

- **Topologies for** $p\pi^+\pi^-$**:**
  $\vec{\gamma}\vec{p} \to p\pi^+$ (missing π^-)
  $\vec{\gamma}\vec{p} \to p\pi^-$ (missing π^+)
  $\vec{\gamma}\vec{p} \to p\pi^+\pi^-$ (no missing particle)
  The observables are weighted avg. over topologies.
- **Topology for** $p\omega$ **(89% branching fraction):**
  $\vec{\gamma}\vec{p} \to p\pi^+\pi^-$(missing π^0)
  Topology identified using Kinematic fitting.
- **Standard cuts & corrections:** vertex cut, photon selection, β cuts, E-p corrections.
- **Event-based method**[1] for signal-background separation.
- **Event-based maximum likelihood method**[2] to fit angular distributions in $\phi_{\text{lab}}^{\text{recoil}}$ and extract the polarization observables.

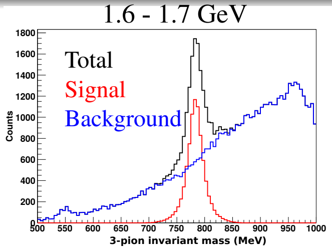

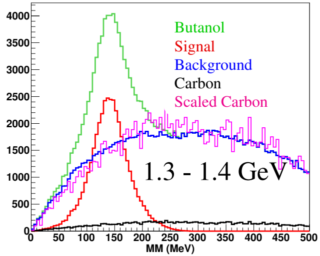

[1] M. Williams *et al.*, JINST 4 (2009) P10003

Data Selection and Analysis

- **Topologies for** $p\pi^+\pi^-$:
  $\vec{\gamma}\vec{p} \to p\pi^+$ (missing π^-)
  $\vec{\gamma}\vec{p} \to p\pi^-$ (missing π^+)
  $\vec{\gamma}\vec{p} \to p\pi^+\pi^-$ (no missing particle)
  The observables are weighted avg. over topologies.
- **Topology for** $p\omega$ **(89% branching fraction):**
  $\vec{\gamma}\vec{p} \to p\pi^+\pi^-$(missing π^0)
  Topology identified using Kinematic fitting.
- **Standard cuts & corrections:** vertex cut, photon selection, β cuts, E-p corrections.
- **Event-based method**[1] for signal-background separation.
- **Event-based maximum likelihood method**[2] to fit angular distributions in $\phi_{\rm lab}^{\rm recoil}$ and extract the polarization observables.

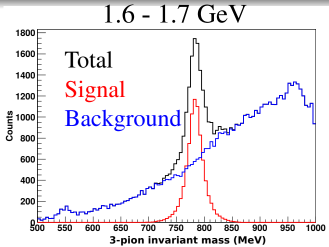

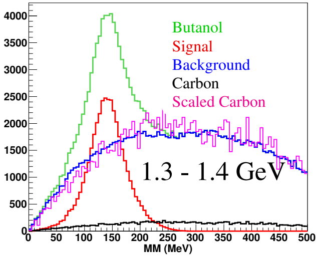

[1] M. Williams *et al.*, JINST 4 (2009) P10003
[2] D G Ireland, CLAS Note 2011-010

Results

Results in $\vec{\gamma}\vec{p} \rightarrow p\omega$

Published Results in $\gamma p \to p\omega$

Isospin filter (sensitive to N^* only), reduces complexity

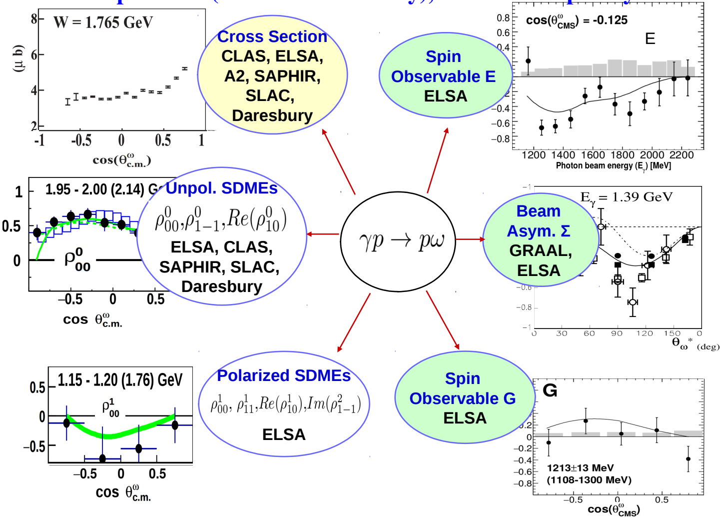

Partial Wave Analysis of $\gamma p \to p\omega$ Observables

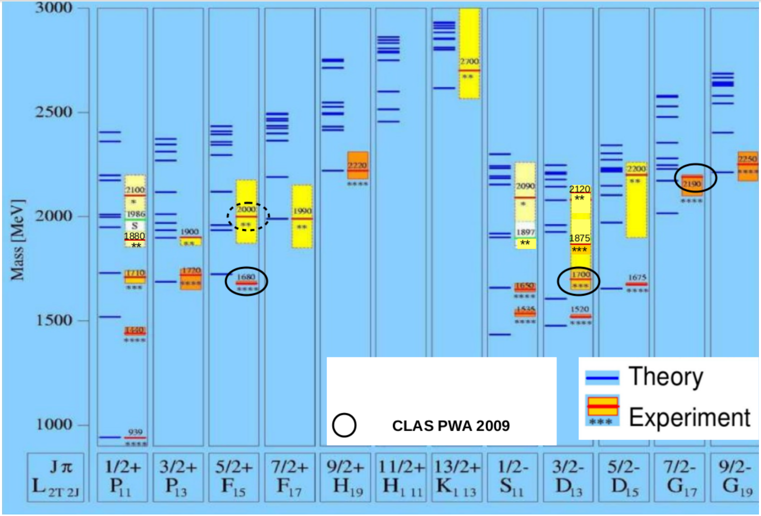

Williams *et al.*, PRC **80**, 065208 (2009)

Partial Wave Analysis of $\gamma p \to p\omega$ Observables

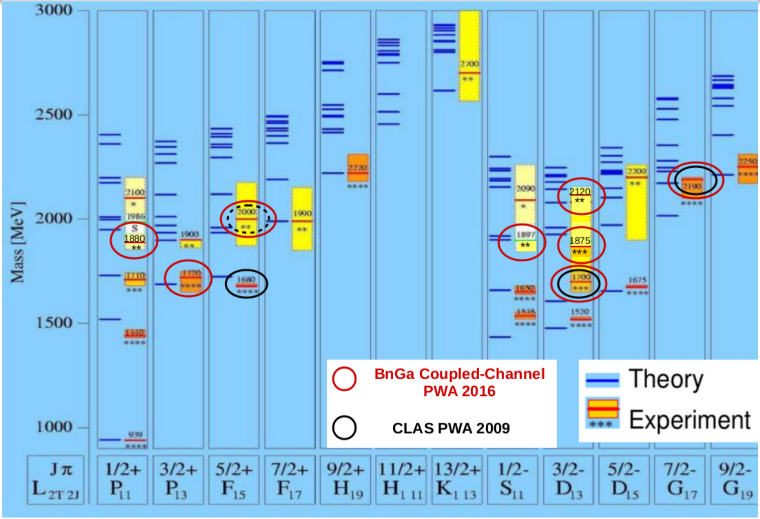

Williams *et al.*, PRC **80** (2009)
Denisenko *et al.*, Phys. Lett. B **755** (2016)

Partial Wave Analysis of $\gamma p \to p\omega$ Observables

Polarized measurements crucial to understand the *t*-channel background: E.g., the BnGa fits above $W = 2$ GeV with pomeron exchange only provided good description for σ_0, but predicted vanishing ρ_{00}, **E**, **Σ**, **G**.

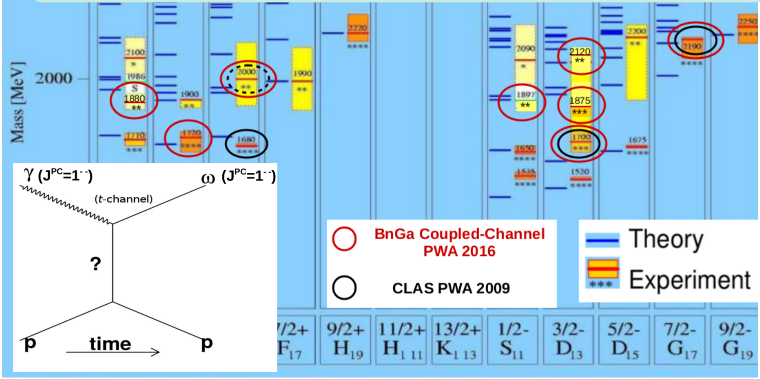

Williams *et al.*, PRC **80** (2009)
Denisenko *et al.*, Phys. Lett. B **755** (2016)

Partial Wave Analysis of $\gamma p \to p\omega$ Observables

The FROST observables will aid in nailing down the resonant contributions, including the resonances above 2 GeV:

- N($\sim$ 2.2 GeV)
  Uncertain J^P:
  $1/2^-$, $3/2^+$, $3/2^-$, or $5/2^+$??
- N($>$ 2.1 GeV) $7/2^-$?

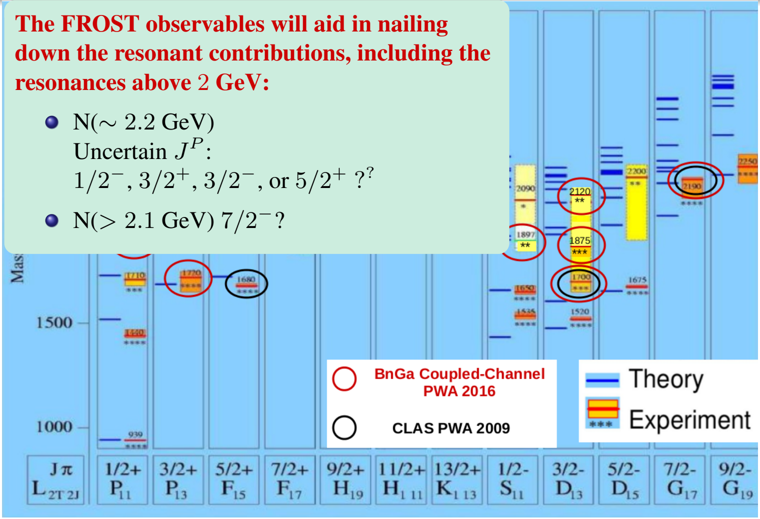

Williams *et al.*, PRC **80** (2009)
Denisenko *et al.*, Phys. Lett. B **755** (2016)

Beam Asymmetry Σ in $\vec{\gamma}p \to p\omega$

ω reconstructed from $\pi^+\pi^-(\pi^0)$

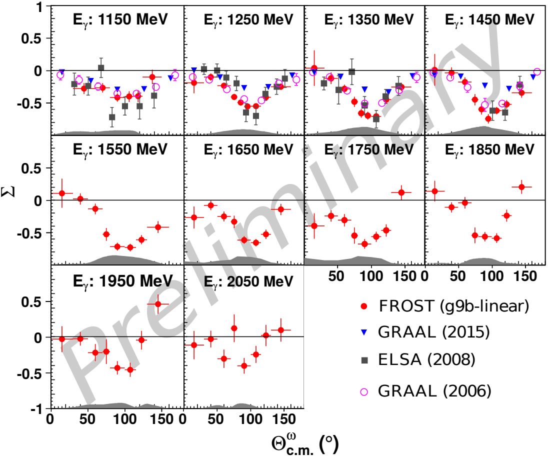

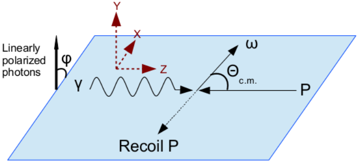

$$\sigma = \sigma_0[1 - \mathbf{\Sigma}\ \delta_l \cos(2\phi)$$
$$+\Lambda\cos(\alpha)(-\delta_l \mathbf{H}\sin(2\phi) + \delta_\odot \mathbf{F})$$
$$-\Lambda\sin(\alpha)(-\mathbf{T} + \delta_l \mathbf{P}\cos(2\phi))$$
$$-\Lambda_z(-\delta_l \mathbf{G}\sin(2\phi) \quad + \quad \delta_\odot \mathbf{E})]$$

$\delta_\odot(\delta_l)$: degree of beam pol.
Λ : degree of target pol.

Beam Asymmetry Σ in $\vec{\gamma}p \to p\omega$

ω reconstructed from $\pi^+\pi^-(\pi^0)$

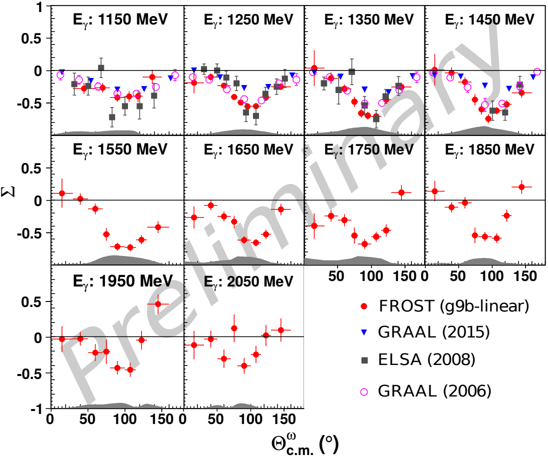

- **FROST**: transversely pol. target (more complex analysis)
  Others: unpolarized H_2 target
- **FROST results** agree well with previously published results except for GRAAL 15.
- First-time high quality measurements at $E_\gamma \in [1.5, 2.1]$ GeV. Large Σ indicate significant s- and/or u-contributions at these energies.

First Measurements of Target Asymmetry T in $\gamma\vec{p} \to p\omega$

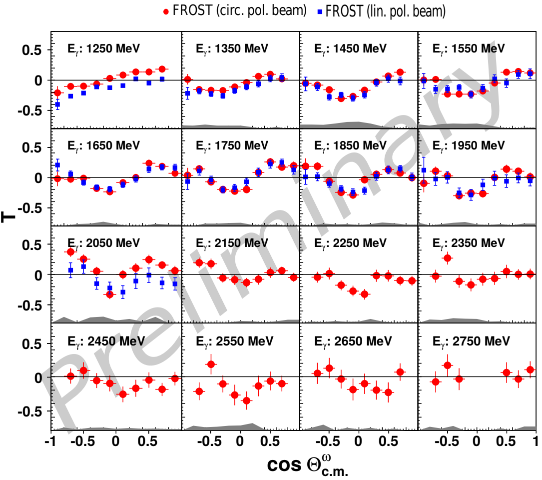

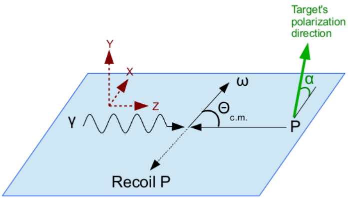

The two experimental results on target asym. **T** from FROST agree well.

$$\sigma = \sigma_0[1 - \mathbf{\Sigma}\,\delta_l \cos(2\phi) + \Lambda\cos(\alpha)(-\delta_l \mathbf{H}\sin(2\phi) + \delta_\odot \mathbf{F}) - \Lambda\sin(\alpha)(-\mathbf{T} + \delta_l \mathbf{P}\cos(2\phi)) - \Lambda_z(-\delta_l \mathbf{G}\sin(2\phi) + \delta_\odot \mathbf{E})]$$

$\delta_\odot(\delta_l)$: degree of beam pol.

Λ : degree of target pol.

Published Results + New Results in $\gamma p \to p\omega$

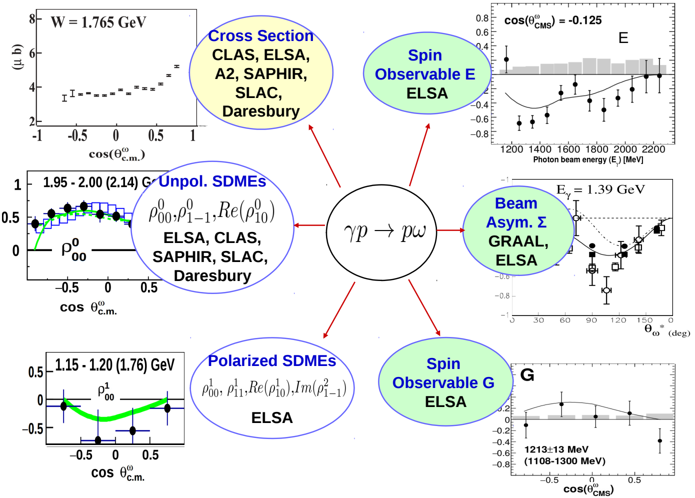

Published Results + New Results in $\gamma p \to p\omega$

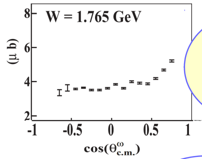

Cross Section
CLAS, ELSA, A2, SAPHIR, SLAC, Daresbury

Spin Observable E
ELSA

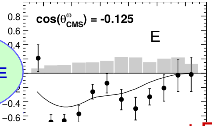

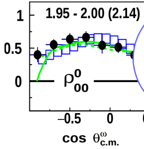

Unpol. SDMEs
$\rho^0_{00}, \rho^0_{1-1}, Re(\rho^0_{10})$
ELSA, CLAS, SAPHIR, SLAC, Daresbury

+ FROST (Prelim.) Results

Beam \ Target	Transversely Pol.	Longitudinally Pol.
Linearly Pol.	Σ, T, H, P	Σ, G
Circularly Pol.	F, T	E

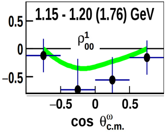

Polarized SDMEs
$\rho^1_{00}, \rho^1_{11}, Re(\rho^1_{10}), Im(\rho^2_{1-1})$
ELSA

Spin Observable G
ELSA

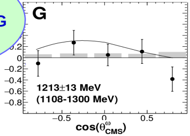

Results

Results in $\vec{\gamma}\vec{p} \to p\pi^+\pi^-$

Published Results in $\vec{\gamma}\vec{p} \to p\pi^+\pi^-$

Allow the study of sequential decays of intermediate N^* and also $N^* \to p\rho$ decay but the large hadronic background makes it challenging.

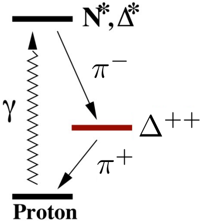

Published Results in $\vec{\gamma}\vec{p} \to p\pi^+\pi^-$

Polarization observables database rather sparse in the past. Moreover, existing models do not describe the data well.

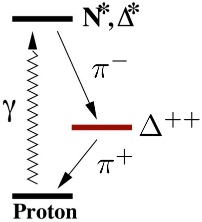

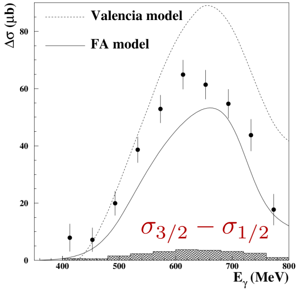

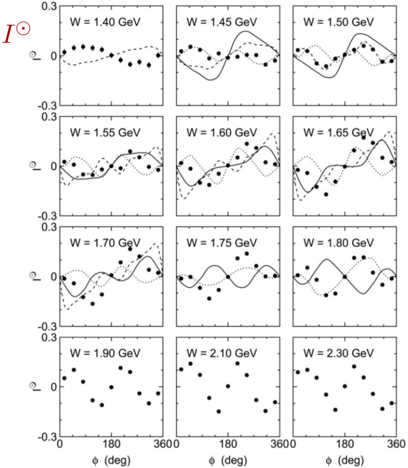

Beam \ Target	Transversely Pol.	Longitudinally Pol.
Linearly Pol.	$P^{s,c}_{x,y}$, $P_{x,y}$, $I^{s,c}$	$P^{s,c}_{z}$, P_{z}, $I^{s,c}$
Circularly Pol.	$P^{\odot}_{x,y}$, $P_{x,y}$, $I^{\odot}$	$P^{\odot}_{z}$, P_{z}, $I^{\odot}$

Strauch *et al.*, PRL **95**, 162003 (2005); Krambrich *et al.*, PRL **103**, 052002 (2009)
Ahrens *et al.*, EPJ A **34**, 11 (2007)

Beam Asymmetry I^s in $\vec{\gamma}p \to p\pi^+\pi^-$

Example: $1.30 < E_\gamma < 1.40$ GeV (Total E_γ range covered: 0.7 - 2.1 GeV)

● FROST (preliminary) ● C. Hanretty *et al.* , CLAS-g8b run (in preparation for publication)

— Fourier sine fit to g8b

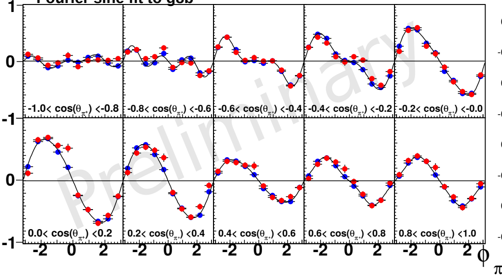

— BnGa fits to I^s, CLAS-g8b run

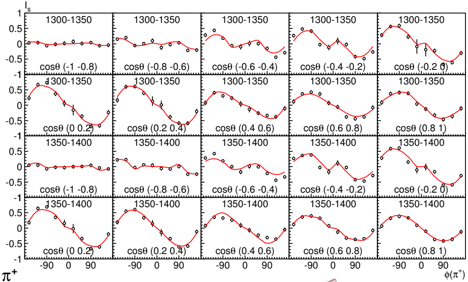

Good agreement between experiments

$$I = I_0\{\delta_l[I^s\sin(2\beta) + I^c\cos(2\beta)]\}$$

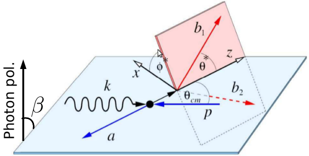

First Measurements of Target Asym. $P_{x,y}$ in $\gamma\vec{p} \to p\pi^+\pi^-$

Example: $0.8 < E_\gamma < 0.9$ GeV (Total E_γ range covered: 0.7 - 2.1 GeV)

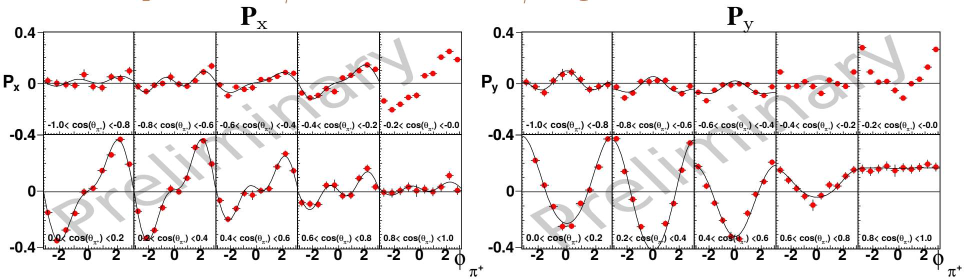

FROST g9b (lin. pol. beam) **Solid curves : Fourier fit ($n < 3$)**

3-dim. phase space: $(E_\gamma, \phi^*_{\pi^+}, \cos\theta^*_{\pi^+})$

$$I = I_0[1 + \Lambda\cos(\alpha)\mathbf{P_x} + \Lambda\sin(\alpha)\mathbf{P_y}]$$

Λ : degree of target pol.

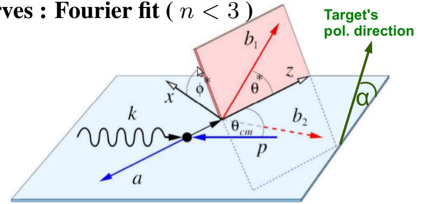

W. Roberts and T. Oed, PRC **71**, 055201 (2005)

First Measurements of P_x^c in $\vec{\gamma}\vec{p} \to p\pi^+\pi^-$

-1.0 $< \cos\theta^*_{\pi^+} <$ **0.0**

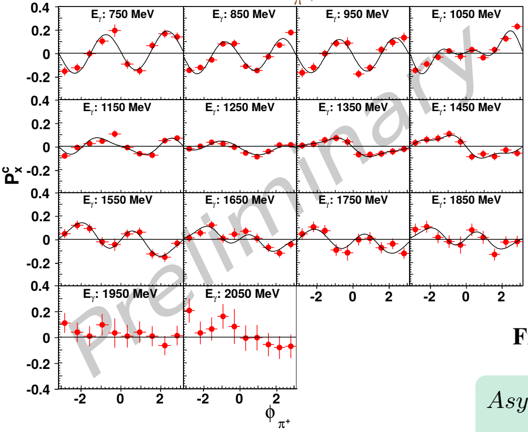

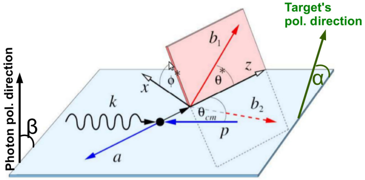

Fine binning in (E_γ, $\phi^*_{\pi^+}$), 2 bins in $\cos\theta^*_{\pi^+}$

FROST g9b (lin. pol. beam)

Solid Line - Fourier fit ($n < 4$ **)**

$$Asym. = \delta_l \Lambda\{\sin2\beta(\mathbf{P^s_x}\cos\alpha + \mathbf{P^s_y}\sin\alpha) + \cos2\beta(\mathbf{P^c_x}\cos\alpha + \mathbf{P^c_y}\sin\alpha)\}$$

$\delta_l(\Lambda)$: degree of beam (target) pol.

First Measurements of P_x^c in $\vec{\gamma}\vec{p} \to p\pi^+\pi^-$

$0.0 < \cos\theta^*_{\pi^+} < 1.0$

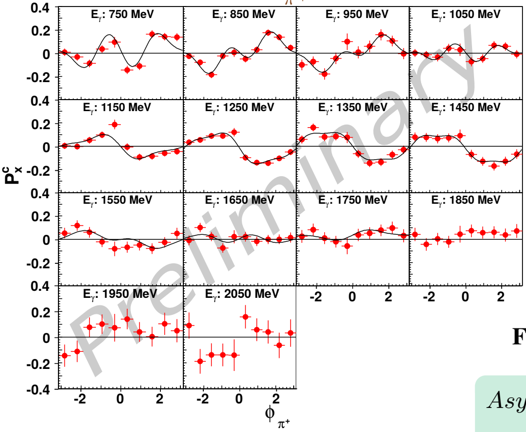

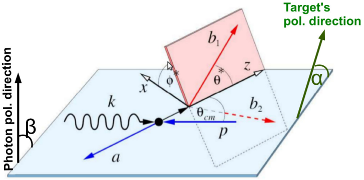

FROST g9b (lin. pol. beam)

Solid Line - Fourier fit ($n < 4$)

Fine binning in (E_γ, $\phi^*_{\pi^+}$), 2 bins in $\cos\theta^*_{\pi^+}$

$$Asym. = \delta_l \Lambda\{\sin 2\beta(\mathbf{P_x^s}\cos\alpha + \mathbf{P_y^s}\sin\alpha) + \cos 2\beta(\mathbf{P_x^c}\cos\alpha + \mathbf{P_y^c}\sin\alpha)\}$$

$\delta_l(\Lambda)$: degree of beam (target) pol.

Outline

1. Introduction
   - Strong Interaction
   - Why Baryon Spectroscopy?
   - Polarization Observables
   - The FROST Experiment using CLAS
2. Data Analysis and Results
   - $\vec{\gamma}\vec{p} \to p\omega$ Reaction
   - $\vec{\gamma}\vec{p} \to p\pi^+\pi^-$ Reaction
3. Outlook

Summary

- **Photoproduction of vector mesons and multi-pion final states**: essential to **discover new resonances** and better understand the known resonances.
- **Many first-time measurements** from CLAS-FROST for $\vec{\gamma}\vec{p} \to p\omega$ (Σ (for $E_\gamma > 1.7$ GeV), T, H, P, F) and $\vec{\gamma}\vec{p} \to p\pi^+\pi^-$ ($I^{s,c}$, $P_{x,y}$, $P^{s,c}_{x,y}$): they will **significantly augment the world database** of polarization observables in photoproduction.
- **The high-quality FROST results are expected to put tight constraints on data interpretation tools**, immensely aiding in determining contributing N^* with minimal ambiguities.
- Our findings from FROST on the N^* members, together with the findings on the strange members (e.g. from PANDA at GSI, BES at Beijing, GlueX at JLab) of the multiplets will complete the study of the light baryon spectrum. This will give more insight into the phenomenon of color confinement in the system of light quarks.

Summary

Several papers in preparation:

- P. Roy, V. Crede *et al.*, "Measurement of the Beam Asymmetry for the ω Photoproduction off the Proton from the FROST Experiment," paper ready for collaboration review.
- P. Roy, V. Crede *et al.*, "Measurement of Single and Double Polarization Asymmetries in ω Photoproduction from FROST," in preparation.
- Paper on BnGa Partial Wave Analysis of the new FROST data, in preparation.
- Z. Akbar, P. Roy, V. Crede *et al.*,"Measurement of the Helicity Asymmetry in $\omega/\eta \to \pi^+\pi^-\pi^0$ Photoproduction," paper ready for collaboration review.
- Several papers on the polarization observables for $\pi^+\pi^-$ photoproduction off the proton.

Acknowledgements

Volker Crede
Hadronic physics group
Committee members
FROST members
My family and friends

Acknowledgements

Volker Crede
Hadronic physics group
Committee members
FROST members
My family and friends

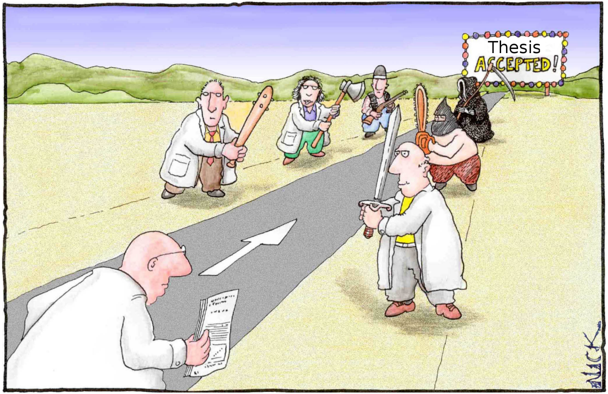

Backup slides

CLAS Experiment Details

Capability	Quantity	Range
Coverage	Charged-particle angle	$8^\circ \leqslant \theta \leqslant 140^\circ$
	Charged-particle momentum	$p \geqslant 0.2$ GeV/c
	Photon angle (4 sectors)	$8^\circ \leqslant \theta \leqslant 45^\circ$
	Photon angle (2 sectors)	$8^\circ \leqslant \theta \leqslant 75^\circ$
	Photon energy	$E_\gamma \geqslant 0.1$ GeV
Resolution	Momentum ($\theta \lesssim 30^\circ$)	$\sigma_p/p \approx 0.5\%$
	Momentum ($\theta \gtrsim 30^\circ$)	$\sigma_p/p \approx$ (1–2)%
	Polar angle	$\sigma_\theta \approx 1$ mrad
	Azimuthal angle	$\sigma_\phi \approx 4$ mrad
	Time (charged particles)	$\sigma_t \approx$ (100–250) ps
	Photon energy	$\sigma_E/E \approx 10\%/\sqrt{E}$
Particle ID	π/K separation	$p \leqslant 2$ GeV/c
	π/p separation	$p \leqslant 3.5$ GeV/c
	π^- misidentified as e^-	$\leqslant 10^{-3}$
Luminosity	Electron beam	$L \approx 10^{34}$ nucleon cm^{-2} s^{-1}
	Photon beam	$L \approx 5 \times 10^{31}$ nucleon cm^{-2} s^{-1}
Data acquisition	Event rate	4 kHz
	Data rate	25 MB/s
Polarized target	Magnetic field	$B_{\max} = 5$ T

CLAS Experiment Details Continued

(1) Electron beam current: $5 - 14$ nA
(2) Electron beam energy: 3.082 GeV (circ. + lin.), 5.078 GeV (circ.)
(3) Gold foil of 10^{-4} radiation length thickness used for creating circularly-polarized photons from longitudinally-polarized electrons. Longitudinally-polarized electrons created by circularly-polarizing the laser using 2 Pockel cells prior to irradiating the GaAs photocathode.
(4) Diamond radiator of thickness 50μm to produce lin. pol. photons. The divergence of the e^- beam in the crystal increases with thickness. More divergence leads to broader coherent peaks and a lower degree of polarization.

(1) E-T plane resolution: 110 ps
(2) Photon tagging resolution: $\Delta(E)/E = 0.1\%$
(3) Start counter resolution: 290 ps at the straight section, 320 ps at the nose
(4) TOF resolution: 80 ps for short counters, 160 ps for the long counters
(5) Average time resolution for reconstructed electrons in CLAS: 150 ps

The Horizontal Dilution Refrigerator

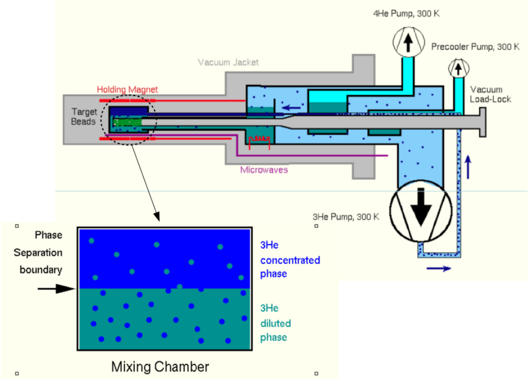

Below 0.8 K, the ^{3}He-^{4}He mixture separated into two phases:
^{3}He rich (specific heat = 22 J/(mol K)),
^{3}He poor (specific heat = 106 J(mol K)).

Due to the difference in the specific heat, ^{3}He absorbs heat from its surrounding while traveling from the concentrated phase to the dilute phase.

Photoproduction Cross Section

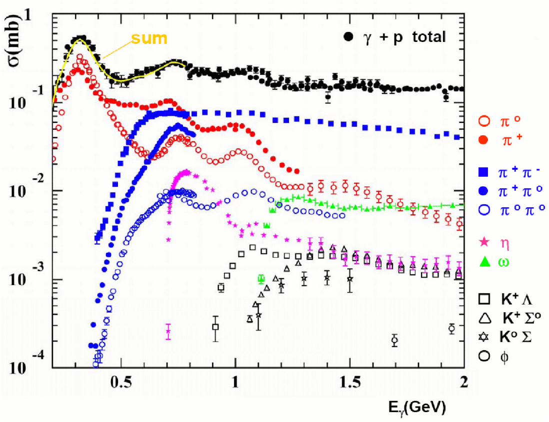

Photon Selection Cuts

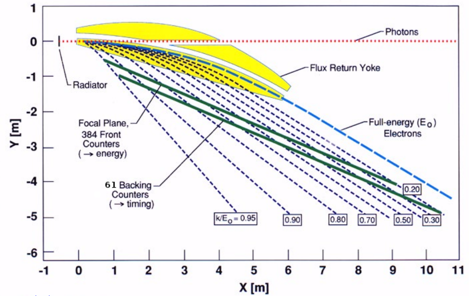

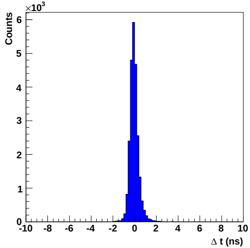

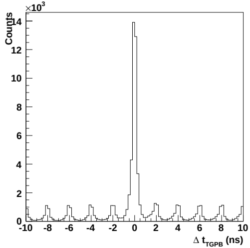

$\Delta(t) = t_{\text{event}} - t_\gamma$

$\sim$ 5 candidate photons per event on average.

Cuts applied:

1) $|\Delta(t)| < 1$ ns

2) Only 1 candidate photon in the same RF bucket and all tracks of the event originate from the same tagged photon ($88 - 90\%$ events).

β cut

$$\beta_{cal} = \frac{p_{DC}}{\sqrt{{p_{DC}}^2 + m^2}}$$

$$\beta_{meas} = \frac{v_{TOF}}{c}$$

$$\Delta\,\beta = \beta_{cal} - \beta_{meas}$$

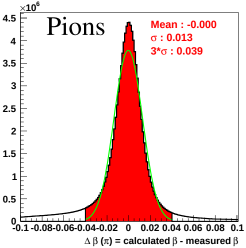

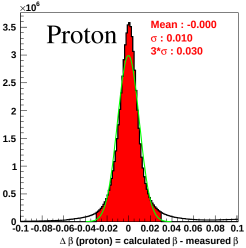

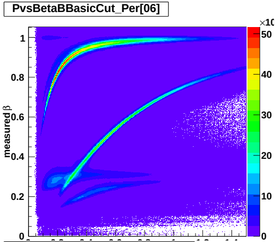

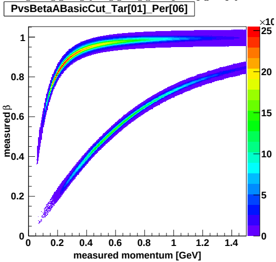

Event Statistics after Various Cuts

Cuts	# of Events (% of Events)			
No cut	1.031e09 (100)			
Vertex Cut (Butanol Events)	6.74e07 (6.5)			
Vertex Cut + Topology Cut	Topology 1	Topology 2	Topology 3	Topology 4
	2.05e07 (1.99)	1.99e07 (1.93)	1.71e07 (1.66)	1.00e07 (0.97)
Vertex Cut + Topology Cut + Photon Selection Cuts	1.16e07 (1.13)	9.83e06 (0.95)	1.12e07 (1.09)	6.30e06 (0.61)
Vertex Cut + Topology Cut + Photon Selection + β Cut	8.43e06 (0.82)	7.72e06 (0.75)	6.54e06 (0.63)	4.01e06 (0.39)

Event-Based Qfactor Method with Likelihood Fits

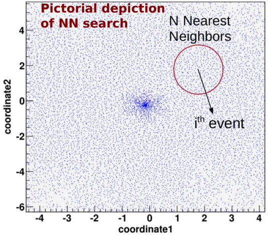

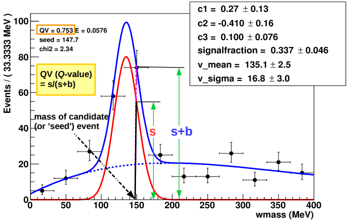

- **A multivariate analysis -** For each event ("seed event"), find N nearest neighbors in $N-$D kinematic phase space (e.g. λ, θ_{HEL}, ϕ_{HEL}, $\cos(\theta^{p})_{c.m.}$, $\phi^{p_{\text{recoil}}}_{\text{c.m.}}$ for ω analysis). Plot mass distribution of the $N+1$ events and fit.
- Since N is small (300), use ML method to fit the mass distribution.
  $L = \prod_i [f^{Signal}(m_i, \alpha) + f^{Bkg}(m_i, \beta)]$

  $\mathbf{Q}_{\mathbf{seed-event}} = \frac{f^{Signal}(m_0, \alpha^{best})}{[f^{Signal}(m_0, \alpha^{best}) + f^{Bkg}(m_0, \beta^{best})]}$, m_0- seed event's mass.

Fenyman Diagrams for 2-pion Photoproduction

Image Source: J. Ahrens *et al.*, EPJ A **34**, 11 (2007).

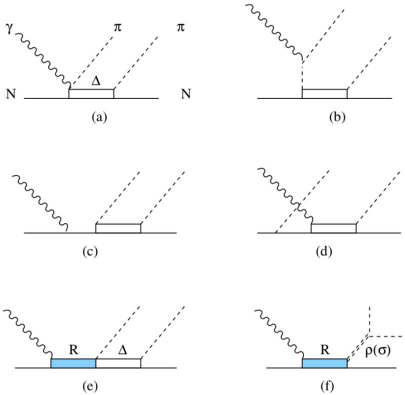

Figure 1.12: Feynman diagrams for two-pion photoproduction. a) Δ-Kroll-Ruderman term, b) Δ pion-pole term, c) Δ exchange term, d) direct Born term, e)-f) resonance terms.

Published Results in $\vec{\gamma}\vec{p} \to p\pi^+\pi^-$

- Allow the study of sequential decays of intermediate N^* and also $N^* \to p\rho$ decay but the large hadronic background makes it challenging.
- Reaction described using 2 planes (5 kinematic variables) $\to$ more spin observables than in single-meson photoproduction using polarized beam and target.

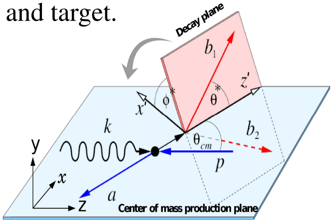

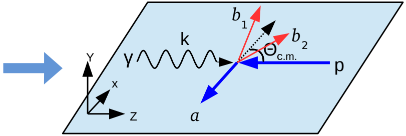

2 beam-pol. observables: I^s, I^c
Unlike only one (Σ observable) in single-meson photoproduction.

I^s vanishes, I^c survives.

W. Roberts and T. Oed, PRC **71**, 055201 (2005)

First Measurements of F in $\vec{\gamma}\vec{p} \to p\omega$

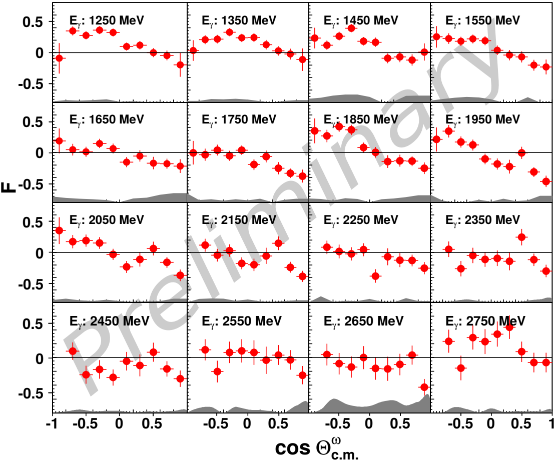

Double-polarization observable F

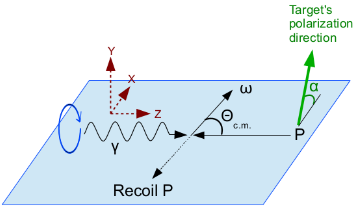

$$\sigma = \sigma_0[1 - \boldsymbol{\Sigma}\ \delta_l \cos(2\phi)$$
$$+\Lambda\cos(\alpha)(-\delta_l \mathbf{H}\sin(2\phi) + \delta_\odot \mathbf{F})$$
$$-\Lambda\sin(\alpha)(-\mathbf{T} + \delta_l \mathbf{P}\cos(2\phi))]$$
$$-\Lambda_z(-\delta_l \mathbf{G}\sin(2\phi) \quad + \quad \delta_\odot \mathbf{E})]$$

$\delta_\odot(\delta_l)$: degree of beam pol.

Λ : degree of target pol.

First Measurements of H in $\vec{\gamma}\vec{p} \to p\omega$

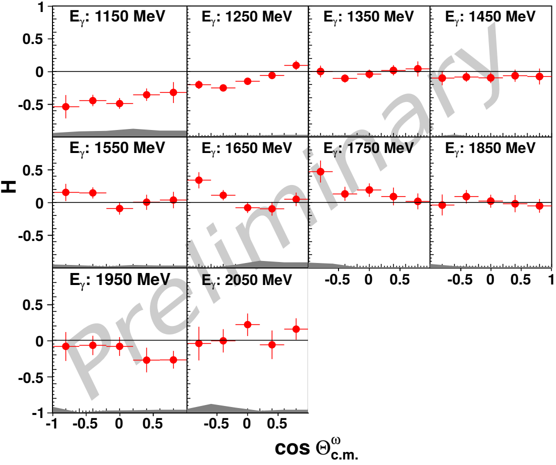

Double-polarization observable H

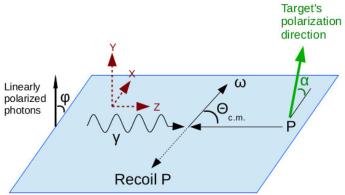

$$\sigma = \sigma_0[1 - \Sigma\,\delta_l \cos(2\phi)$$
$$+\Lambda\cos(\alpha)(-\delta_l \mathbf{H}\sin(2\phi) + \delta_\odot \mathbf{F})$$
$$-\Lambda\sin(\alpha)(-\mathbf{T} + \delta_l \mathbf{P}\cos(2\phi))]$$
$$-\Lambda_z(-\delta_l \mathbf{G}\sin(2\phi) \quad + \quad \delta_\odot \mathbf{E})]$$

$\delta_\odot(\delta_l)$: degree of beam pol.
Λ : degree of target pol.

First Measurements of P in $\vec{\gamma}\vec{p} \rightarrow p\omega$

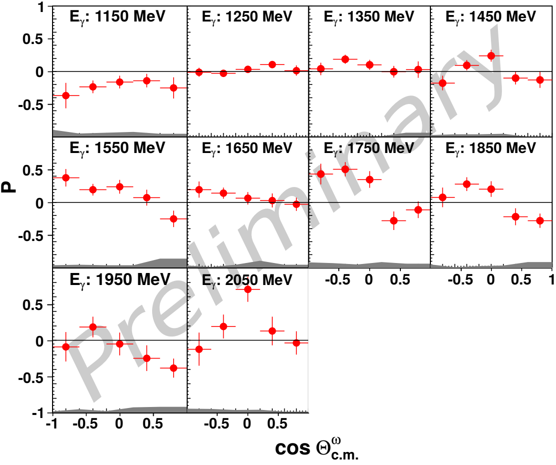

Double-polarization observable P

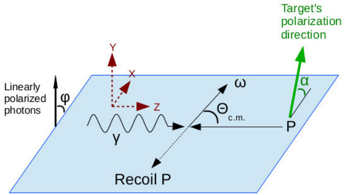

$$\sigma = \sigma_0[1 - \mathbf{\Sigma}\, \delta_l \cos(2\phi)$$
$$+\Lambda\cos(\alpha)(-\delta_l \mathbf{H}\sin(2\phi) + \delta_\odot \mathbf{F})$$
$$-\Lambda\sin(\alpha)(-\mathbf{T} + \delta_l \mathbf{P}\cos(2\phi))]$$
$$-\Lambda_z(-\delta_l \mathbf{G}\sin(2\phi) \quad + \quad \delta_\odot \mathbf{E})]$$

$\delta_\odot(\delta_l)$: degree of beam pol.

Λ : degree of target pol.

Beam Asymmetry I^c in $\vec{\gamma} p \to p\pi^+\pi^-$

Example: $1.30 < E_\gamma < 1.40$ GeV

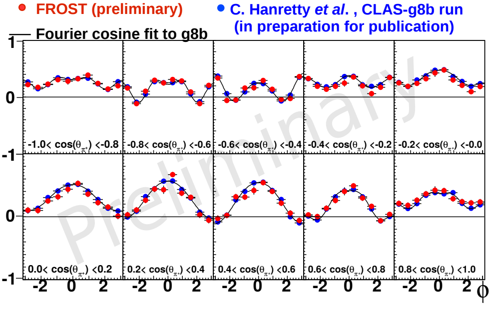

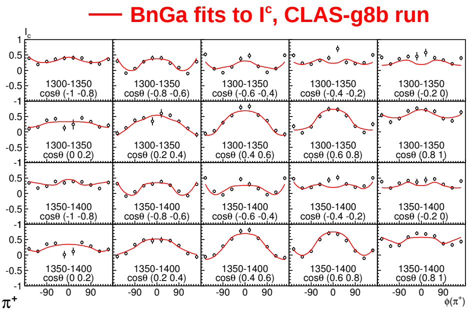

Good agreement between experiments

$$I = I_0\{\delta_l[I^s \sin(2\beta) + I^c \cos(2\beta)]\}$$

Systematic Errors

Systematics	$\lvert \Delta$ Obs./Obs.$\rvert$ (%)		
	g9b-lin.		g9b-circ.
	$\gamma p \to p\,\pi^+\pi^-$	$\gamma p \to p\,\omega$	$\gamma p \to p\,\omega$
Q-factor method	10	4-5 (threshold E_γ)	4-5 (threshold E_γ)
		7-9 (higher E_γ)	7-9 (higher E_γ)
Beam-polarization	5	5	4
Target-polarization	2	2	2
Target-offset angle	2	2	2
Normalization	5	5	2
Beam-charge asym.	-	-	< 0.2
Accidental photons	Unknown	Unknown	Unknown
σ_{total}	13	9 (threshold E_γ)	7 (threshold E_γ)
		12 (higher E_γ)	11 (higher E_γ)

Why are Spin Observables Important?

[1] R. Bradford *et al.* (CLAS), PRC **75**, 035205 (2007), Observables C_x, C_z from $\vec{\gamma}p \rightarrow K^+\vec{\Lambda}$
[2] Fits: BnGa Model, V.A. Nikonov *et al.*, Phy. Lett. B **662**, 245 (2008)

C_x, C_z Fits without N(1900)$3/2^+$ resonance

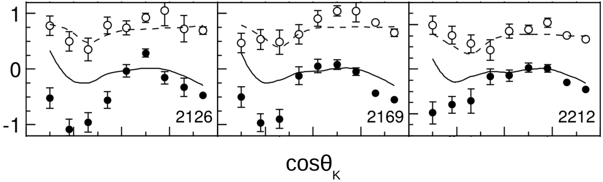

C_x, C_z Better Fit Results with N(1900)$3/2^+$!

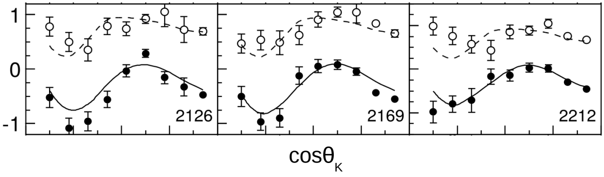

Currently 17 N^* and 10 Δ^* with at least (∗∗∗) rating.

N^*	J^P ($L_{2I,2J}$)	2010	2012
$N(1440)$	$1/2^+$ (P_{11})	∗∗∗∗	∗∗∗∗
$N(1520)$	$3/2^-$ (D_{13})	∗∗∗∗	∗∗∗∗
$N(1535)$	$1/2^-$ (S_{11})	∗∗∗∗	∗∗∗∗
$N(1650)$	$1/2^-$ (S_{11})	∗∗∗∗	∗∗∗∗
$N(1675)$	$5/2^-$ (D_{15})	∗∗∗∗	∗∗∗∗
$N(1680)$	$5/2^+$ (F_{15})	∗∗∗∗	∗∗∗∗
$N(1685)$			∗
$N(1700)$	$3/2^-$ (D_{13})	∗∗∗	∗∗∗
$N(1710)$	$1/2^+$ (P_{11})	∗∗∗	∗∗∗
$N(1720)$	$3/2^+$ (P_{13})	∗∗∗∗	∗∗∗∗
$N(1860)$	$5/2^+$		∗∗
$N(1875)$	$3/2^-$		∗∗∗
$N(1880)$	$1/2^+$		∗∗
$N(1895)$	$1/2^-$		∗∗
$N(1900)$	$3/2^+$ (P_{13})	∗∗	∗∗∗
$N(1990)$	$7/2^+$ (F_{17})	∗∗	∗∗
$N(2000)$	$5/2^+$ (F_{15})	∗∗	∗∗
~~$N(2080)$~~	D_{13}	∗∗	
~~$N(2090)$~~	S_{11}	∗	
$N(2040)$	$3/2^+$		∗
$N(2060)$	$5/2^-$		∗∗
$N(2100)$	$1/2^+$ (P_{11})	∗	∗
$N(2120)$	$3/2^-$		∗∗
$N(2190)$	$7/2^-$ (G_{17})	∗∗∗∗	∗∗∗∗
~~$N(2200)$~~	D_{15}	∗∗	
$N(2220)$	$9/2^+$ (H_{19})	∗∗∗∗	∗∗∗∗

Scattering Amplitudes in $\gamma p \to p\pi^+\pi^-$ and $\gamma p \to p\omega$

$\gamma p \to p\pi^+\pi^-$ reaction: Roberts and Oed, PRC **71**, 055201 (2015)

- 8 independent helicity amplitudes after parity invariance operation.
- Need 15 carefully selected observables at each kinematic bin for fully determining the helicity amplitudes.
- A complete measurement will require certain single, double and triple polarization observables in addition to the differential cross section.

$\gamma p \to p\omega$ reaction: Pichowsky *et al.*, PRC **53** (1996)

- 12 independent helicity amplitudes after parity invariance.
- 8 single spin, 51 double spin, 123 triple spin and 108 quadrupole spin (γ, p, $p^{'}$, vector and tensor pol. of ω) observables after parity conservation.
- Need 23 carefully selected observables for determining the helicity amplitudes.
- A complete experiment doesn't seem plausible, but it is useful to extract experimental observables to extract useful dynamical information.

Multiplets in the 2^{nd} excitation band of N^*

V. Crede and W. Roberts, Rept.Prog.Phys. **76** (2013)

$SU(6)$ (flavor + spin), $O(3)$: orthogonal group of rotations
$6 \otimes 6 \otimes 6 = 56_S \oplus 70_M \oplus 70_M \oplus 20_A$
$56 = 10^4 \oplus 8^2, (4 = 2(\frac{3}{2}) + 1)$
$70 = 10^2 \oplus 8^4 \oplus 8^2 \oplus 1^2$
$20 = 8^2 \oplus 1^4$

Why is 20plet inconsistent with the static quark-diquark picture?
The static diquark: $6 \otimes 6 = 21 \oplus 15$
The symmetry of diquark requires it to be 21 since the color $\Psi$is antisymmetric.
The static diquark +the third quark: $21 \otimes 6 = 56 \oplus 70$, i.e. no 20plet!

Only two N^*states with 1-star rating have been assigned to the 20plet.

Light Baryon Spectroscopy

Naming light baryons: Symbol (Mass in MeV/c^2) J^P

- **Baryon with 0 s quark**: N if $I = 1/2$, Δ if $I = 3/2$.
- With 1 s quark: Λ if $I = 0$, Σ if $I = 1$.
- With 2 s quarks: Ξ. It has $I = 1/2$.
- With 3 s quarks: Ω. It has $I = 0$.

Light Baryon Spectroscopy

The **ground state** of light baryons can be grouped in multiplets.

- Baryons with $J^P = \frac{1}{2}^+$ in an octet.
- Baryons with $J^P = \frac{3}{2}^+$ in a decuplet.

All of them have been experimentally observed.

Naming light baryons: Symbol (Mass in MeV/c^2) J^P

- **Baryon with 0 s quark**: N if $I = 1/2$, Δ if $I = 3/2$.
- With 1 s quark: Λ if $I = 0$, Σ if $I = 1$.
- With 2 s quarks: Ξ. It has $I = 1/2$.
- With 3 s quarks: Ω. It has $I = 0$.

Baryon octet

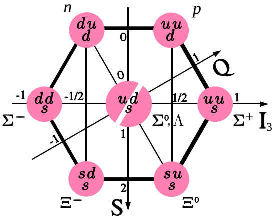

Baryon decuplet

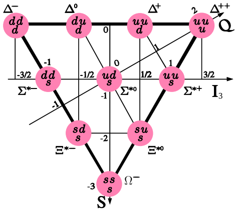

A CQM Prediction for the N^* Spectrum

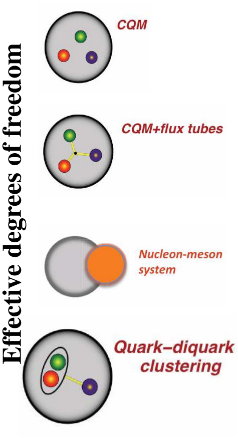

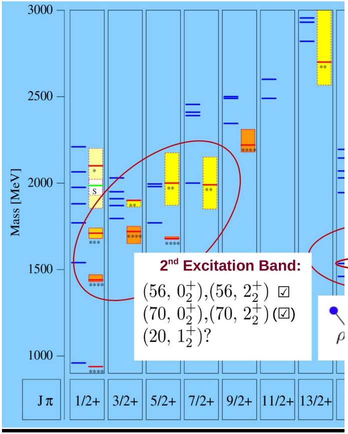

N^*	J^P $(L_{2I,2J})$	2010	2012
$N(1440)$	$1/2^+$ (P_{11})	****	****
$N(1520)$	$3/2^-$ (D_{13})	****	****
$N(1535)$	$1/2^-$ (S_{11})	****	****
$N(1650)$	$1/2^-$ (S_{11})	****	****
$N(1675)$	$5/2^-$ (D_{15})	****	****
$N(1680)$	$5/2^+$ (F_{15})	****	****
$N(1685)$			*
$N(1700)$	$3/2^-$ (D_{13})	***	***
$N(1710)$	$1/2^+$ (P_{11})	***	***
$N(1720)$	$3/2^+$ (P_{13})	****	****
$N(1860)$	$5/2^+$		**
$N(1875)$	$3/2^-$		***
$N(1880)$	$1/2^+$		**
$N(1895)$	$1/2^-$		**
$N(1900)$	$3/2^+$ (P_{13})	**	***
$N(1990)$	$7/2^+$ (F_{17})	**	**
$N(2000)$	$5/2^+$ (F_{15})	**	**
~~$N(2080)$~~	D_{13}	**	
~~$N(2090)$~~	S_{11}	*	
$N(2040)$	$3/2^+$		*
$N(2060)$	$5/2^-$		**
$N(2100)$	$1/2^+$ (P_{11})	*	*
$N(2120)$	$3/2^-$		**
$N(2190)$	$7/2^-$ (G_{17})	****	****
~~$N(2200)$~~	D_{15}	**	
$N(2220)$	$9/2^+$ (H_{19})	****	****

The Unbinned Maximum Likelihood Method (MLM)

- The ϕ_{lab} asymmetry was manifested as modulations.

E.g. Asymmetry, $A = \frac{N_\omega(\Rightarrow,+) - N_\omega(\Rightarrow,-)}{N_\omega(\Rightarrow,+) + N_\omega(\Rightarrow,-)}$

Data integrated over all kinematic bins.

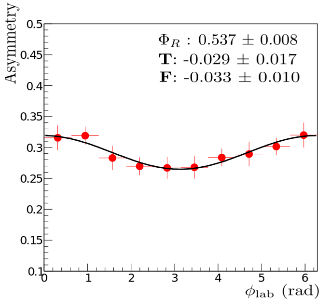

The Unbinned Maximum Likelihood Method (MLM)

- The ϕ_{lab} asymmetry was manifested as modulations.
- Polarization observables were extracted by fitting the modulations using unbinned MLM. **Advantage**: no loss of information due to binning.

$$-\ln L = -\sum_{i=1}^{N_{\text{total}}} w_i \ln\left(P\left(\text{event}_i\right)\right), \; A = \frac{(n_{\text{pol1}} - n_{\text{pol2}})}{(n_{\text{pol1}} + n_{\text{pol2}})},$$

$$\text{where } P\left(\text{event}_i\right) = \begin{cases} \frac{1}{2}(1 + A), & \text{for pol1}, \\ \frac{1}{2}(1 - A), & \text{for pol2 (orthogonal to pol1).} \end{cases}$$

- A was a function of the polarization observable. Minimizing $-\ln L$ gave the most likely value of the observable.

The Unbinned Maximum Likelihood Method (MLM)

- The ϕ_{lab} asymmetry was manifested as modulations.
- Polarization observables were extracted by fitting the modulations using unbinned MLM. **Advantage**: no loss of information due to binning.

$$-\ln L = -\sum_{i=1}^{N_{\text{total}}} w_i \ln\left(P\left(\text{event}_i\right)\right), \; A = \frac{(n_{\text{pol1}} - n_{\text{pol2}})}{(n_{\text{pol1}} + n_{\text{pol2}})},$$

$$\text{where } P\left(\text{event}_i\right) = \begin{cases} \frac{1}{2}(1 + A), & \text{for pol1}, \\ \frac{1}{2}(1 - A), & \text{for pol2 (orthogonal to pol1).} \end{cases}$$

- A was a function of the polarization observable. Minimizing $-\ln L$ gave the most likely value of the observable.